AIAA JOURNAL
Vol. 37, No. 9, September 1999

Decay of Fluctuating Wall-Pressure Field of Mach 5 Turbulent Boundary Layer

Ö. H. Ünalmis* and D. S. Dolling†
University of Texas at Austin, Austin, Texas 78712-1085

The fluctuating wall-pressure field of a nominally two-dimensional, zero-pressure gradient, adiabatic, turbulent boundary layer on the floor of a Mach 5 blowdown tunnel has been investigated experimentally. Various procedures are examined for scaling the streamwise decay of the maximum cross-correlation coefficient of the fluctuating wall-pressure signals with increasing streamwise spacing. For small streamwise separations less than about five boundary-layer thicknesses, the available data from this and other studies can be collapsed in terms of streamwise distance normalized by boundary-layer thickness. For larger separations the database is too sparse to draw a definitive conclusion. The maximum cross-correlation coefficient for incompressible, subsonic, and supersonic boundary layers can be collapsed in terms of a Strouhal number, for Strouhal numbers greater than about 5. In this case the Strouhal number is based on streamwise separation distance, narrowband frequency, and structure convection velocity within that narrow band. Fluctuating pitot-pressure measurements were also made and analyzed in conjunction with hot-wire data obtained in the same facility and with hot-wire experiments at Mach 3. The boundary-layer large-scale structure angles, spanwise scale, and intermittency distributions agree well with results at Mach 3. Based on the higher values of the cross-correlation coefficient in the Mach 5 flow, it appears that turbulent structures are somewhat larger than those at Mach 3.

Nomenclature

d = transducer diameter
f = frequency, Hz
H = boundary-layer shape factor, $\equiv \delta^*/\theta$
h = pitot probe height above wall
M = Mach number
n = velocity power law exponent
P = instantaneous pressure
$R[\,]$ = cross-correlation coefficient
Re = Reynolds number
Re_θ = Reynolds number based on momentum thickness
T = temperature
U = local mean velocity
U_c = convection velocity
U_τ = friction velocity, $\equiv \sqrt{(\tau_w/\rho_w)}$
X = streamwise coordinate
Y = vertical coordinate
Z = spanwise coordinate
ΔX = streamwise separation
ΔY = vertical separation
ΔZ = spanwise separation
δ_0 = boundary-layer velocity thickness, $.99U_\infty$
δ^* = boundary-layer displacement thickness
θ = boundary-layer momentum thickness
λ = wavelength
ν = kinematic viscosity
ξ = smallest separation between transducers, 0.115 in. (2.92 mm)
Π = wake strength
ρ = density
τ = time delay or shear stress
ω = wave-number frequency, $\equiv 2\pi f_c$

Subscripts

w = wall condition
0 = stagnation condition
∞ = freestream condition

Superscript

$+$ = normalized by boundary-layer inner variables

Introduction

OVER the past 40 years there have been many investigations of the fluctuating wall-pressure field under a turbulent boundary layer. These studies have provided the theoretical background and experimental data needed for the solution of some challenging engineering problems, such as the prediction of cabin noise produced by the boundary layer on an aircraft fuselage. To date, most of the experimental studies have been done in incompressible or subsonic flows. Compared to that for the incompressible boundary layer, the database for the compressible boundary layer is rather sparse, and therefore the properties of the fluctuating wall-pressure field for compressible flow are less clear. One essential reason for this is the difficulties (spatial resolution, bandwidth, etc.) of making accurate measurements in high-speed flows.

One distinguishing feature of supersonic/hypersonic boundary-layer turbulence appears to be the long streamwise decay of the large-scale structures. The few available data suggest that the decay distance increases with Mach number. Chyu and Hanly[1] made fluctuating wall-pressure measurements on an ogive cylinder at Mach numbers from 1.6 to 2.5 and observed that for a fixed streamwise separation distance between transducers the peak cross-correlation coefficient increased with Mach number. It appears that the pressure-producing eddies do not have enough time to lose their identities and, consequently, remain coherent for wider separations. Owen and Horstmann[2] and Owen et al.[3] made extensive two-point cross-correlation measurements with hot wires at Mach 7.2 and from space-time correlations concluded that "larger eddies persist for downstream distances of the order of 50 δ_0."

Experimental work by Smits et al.[4] indicates that the turbulence structure of subsonic and supersonic boundary layers differ in some interesting ways, such as in the streamwise length scales derived from space-time correlations, in the intermittency function, and in the dynamics of the large-scale structures. They noted that "the

Received 2 June 1998; revision received 22 January 1999; accepted for publication 8 February 1999.

*Postdoctoral Fellow, Center for Aeromechanics Research, Department of Aerospace Engineering and Engineering Mechanics. Member AIAA.

†Professor, Center for Aeromechanics Research, Department of Aerospace Engineering and Engineering Mechanics. Associate Fellow AIAA.

large-scale structures in the subsonic boundary layer also appear to move slightly slower, and lean more towards the wall, than those observed in supersonic flows, and their shear stress content is distributed differently among the four quadrants." A recent review by Spina et al.[5] discusses what is known and what is not known about supersonic turbulent boundary-layer structure. They point out that for moderate Mach numbers the outer region of the boundary layer is dominated by the entrainment process rather than by turbulence production, and therefore the available studies of supersonic turbulent boundary-layer structure are primarily relevant to the processes by which the boundary layer grows. This is in contrast to subsonic boundary-layer studies, where the focus has largely been on the near-wall turbulence production processes. Additionally, whereas supersonic experiments have been conducted at very high Reynolds numbers, the majority of subsonic research has been at quite low Reynolds numbers. Therefore, definitive statements about the differences between subsonic and supersonic boundary layers are not easy to make.

Other distinguishing features of supersonic large-scale structures are as follows. In a study at Mach 3, Spina et al.[5] found that the onset of intermittency was closer to the boundary-layer edge than in incompressible flow. The average structure angle ranged from 45 to 60 deg across most of the Mach 3 boundary layer with a decrease near the wall and an increase near the boundary-layer edge. They also report that, based on hot-wire results and schlieren photography, the structures convect downstream at approximately 90% of the freestream velocity, and outer-region space-time correlations suggest that the spanwise extent of the largest eddies in the Mach 3 turbulent boundary layer is approximately half of the boundary-layer thickness. The streamwise scales in the same boundary layer were found to be about twice those of incompressible turbulent boundary layers, which "seems to be the most significant structural difference between the two flows—incompressible and compressible—yet found, although both Reynolds number and compressibility could be responsible."[5]

The primary objective of the current work was to examine the fluctuating wall-pressure field under a Mach 5 turbulent boundary layer. Of particular interest is the "turnover" time (or "lifetime") of the large, pressure-generating structures and appropriate methods for scaling their streamwise decay. In addition, to assist in the explanation of the results and for comparison with data from other compressible boundary layers (notably the work at Mach 3 and 7 just discussed), single and dual-channel fluctuating pitot pressures were measured, and hot-wire data obtained in the same facility were examined.

Experimental Program

Wind-Tunnel and Flow Conditions

All of the experiments were conducted in the Mach 5 blowdown tunnel of the University of Texas at Austin. The constant-area test section is 6 in. (15.2 cm) wide × 7 in. (17.8 cm) high and has a length of 12 in. (30.5 cm). Removable side doors allow access to an instrumented floor section. A total of about 140 ft^3 (4 m^3) of compressed air is provided by a Worthington HB4 four-stage compressor and stored in external tanks at a pressure of about 2500 psia (17.24 MPa). Two 420 kW banks of nichrome wire resistive heaters located upstream of the stagnation chamber heat the incoming air to the desired stagnation temperature, which is measured by a Type J thermocouple. The stagnation pressure and temperature for the present experiments were 325 psia (2.24 MPa) (±1%) and 356 K (±1%), respectively. With these stagnation conditions stable run times of up to 1 min could be obtained. The freestream Mach number, velocity, and unit Reynolds number were 4.95, 768 m/s, and 48×10^6/m, respectively. The incoming turbulent boundary layer undergoes natural transition and develops under approximately adiabatic wall conditions.

Instrumentation

Fluctuating wall-pressure measurements were made using Kulite Semiconductor Products, Inc., Model XCQ-062-15A and XCQ-062-50A transducers. These transducers have a nominal outer diameter of 0.0625 in. (0.159 cm) and a pressure-sensitive diaphragm of 0.028-in. (0.071-cm) diam. Based on transducer outer diameter, $d^+ (\equiv du_\tau/\nu_w)$ is about 120. Perforated screens above the diaphragms protect them from damage caused by any dust particles in the flow but limit the frequency response of both models to about 50 kHz. With the assumption that large-scale structures in the boundary layer may range from 1 to $4\delta_0$ in extent, the characteristic frequency range of these structures will be

$$\frac{U_\infty}{1\text{–}4\delta_0} \approx 12\text{–}50\,\text{kHz}$$

Fluctuating pitot-pressure measurements were made using three different probe designs: two single-tipped probes and a double-tipped probe. One of the single-tipped probes and the double-tipped probe could be inserted into the test section through the tunnel ceiling and moved vertically during a run. This allows a user to take multiple segments of data at different vertical positions in a single run. The manual drive mechanism provides 1 in. of travel per 40 turns. A dial gauge, which is accurate to 0.001 in. (0.025 mm), was used to determine probe position. A Kulite Model XCQ-062-100A miniature pressure transducer installed in a tapered stainless-steel tube was used in the single probe. Its tip protrudes 0.05 in. (1.3 mm) upstream of the steel tube.

The double-tipped probe has two Kulite Model XCQ-062-50A miniature pressure transducers. The installation of the transducers is the same as that of the single probe just described. The vertical separation between the probe tip centers is 0.165 in. (4.2 mm). The second single probe projects through the tunnel floor and has a shaft of wedge cross section (wedge angle is smaller than 5 deg) to help minimize interference. This probe cannot be moved during a run, but its height above the floor can be changed between two runs. The center of the transducer could be placed vertically from 0.2 to 2.25 in. (0.51 to 5.72 cm) above the tunnel floor.

All fluctuating pressure transducers were calibrated statically at least on a daily basis, using a Heise digital pressure gauge (Model 710A) accurate to 0.001 psia.

Data Acquisition

Output from the Kulite pressure transducers was amplified by either Dynamics (Model 7525), Vishay Measurements Group (Model 2311), or PARC (Model 113) amplifiers. The amplified signals were then filtered using Ithaco (Models 4113 or 4213) analog filters. The filter cutoff was generally set at 50 kHz, although some additional tests were made at lower settings. For large streamwise transducer separations low sampling rates (200 kHz) were chosen to capture more common "events" over the longer time duration. For spanwise measurements and small streamwise separations high sampling rates (up to 1 MHz) were used to provide good timing resolution for cross correlations. The signal-to-noise ratio was about 100 in most of the cases but overall ranged from 50 to 150.

Data were acquired using two LeCroy analog-to-digital (A/D) converters with 12-bit resolution (Model 6810 waveform recorders). Each A/D converter has 4 megabytes of memory and can sample one channel of data at rates up to 5 MHz or four channels of data simultaneously at rates up to 1 MHz per channel. The two A/D converters can acquire data from eight channels simultaneously when triggered using the same clock. In the current work usually either 262,144 or 524,288 data points per channel were acquired. All data analysis was performed on an HP 9000 Series 380 computer.

Test Program

The experiments can essentially be divided into two parts: fluctuating wall-pressure measurements and fluctuating pitot-pressure measurements. A schematic of the various experimental arrangements is given in Fig. 1. For fluctuating wall-pressure measurements a circular brass plug was installed with its instrumented surface flush with the tunnel floor. This plug has a row of 26 transducer ports on its centerline, and the distance between consecutive ports is 0.115 in. (0.292 cm ≈ $0.2\delta_0$). With the help of two additional smaller plugs at different locations in the floor, it was possible to obtain data over a range of streamwise separation distances from 0.2 to $28\delta_0$ (Fig. 1a). Rotating the circular plug by 90 deg made it possible to perform spanwise measurements and obtain data over a range of spanwise spacings from 0.2 to $4\delta_0$ (Fig. 1b). In addition, measurements were

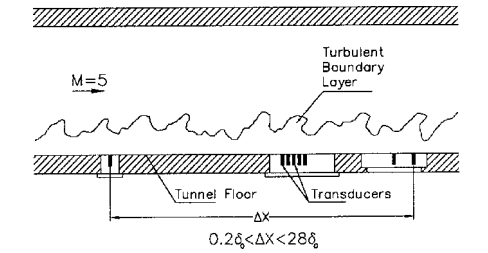

a)

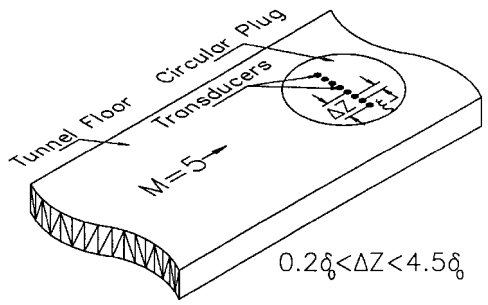

b)

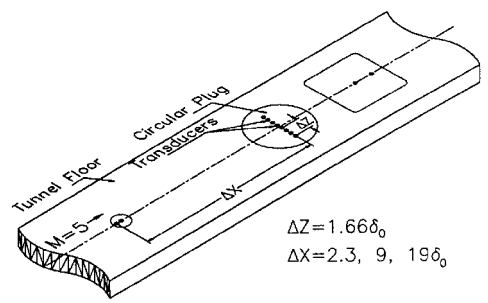

c)

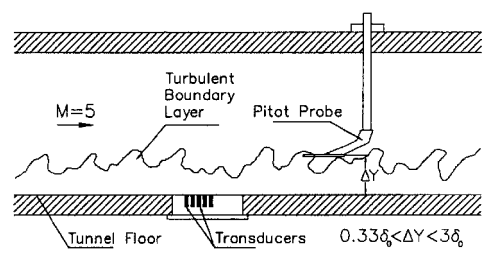

d)

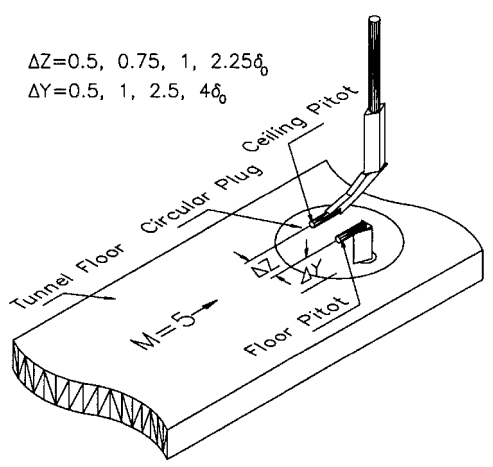

e)

Fig. 1 Schematic of experiments: a), b), and c) show fluctuating wall-pressure measurements; and d) and e) show fluctuating pitot-pressure measurements.

also obtained using transducers separated in both streamwise and spanwise directions (Fig. 1c).

Single pitot experiments were conducted at several vertical locations from 0.3 to $4\delta_0$ (Fig. 1d). These data were used to determine the intermittency profile across the boundary layer. Two-point measurements were made using the double-tipped probe at several stations across the boundary layer. The inclination angles of the large-scale boundary layer were determined using these data.

Another set of pitot experiments employed the two independent single-tipped pitot probes, one projecting through the floor and the other through the ceiling (Fig. 1e). The tips of the transducers in these two probes were located at the same streamwise and vertical position, and the spanwise separation distance between the probes was changed for each experiment. This was done for several vertical positions inside and outside the boundary layer. The purpose of these experiments was to determine the spanwise length scale of the large-scale boundary-layer structures within the boundary layer and the reference no-correlation level in the freestream.

Mean Boundary-Layer Properties

The incoming velocity profile derived from pitot probe measurements is shown in Fig. 2 (Ref. 6). Static pressure and total temperature were assumed constant through the boundary layer in the computation of this profile. The profile is a good fit to a power law with an exponent of $n = 9.5$, which is consistent with a compilation of data of n vs Re_θ given by Settles.[7] To determine the skin-friction coefficient C_f and the wake strength parameter Π, the data were fitted to the law of the wall/law of the wake using the method of Sun and Childs.[8] Good fits were obtained, an example of which is shown in Fig. 3 (Ref. 9). The boundary-layer thickness δ_0 is based on the height in the boundary layer where the mean velocity reaches 99% of the freestream value, unless specified otherwise. Values of

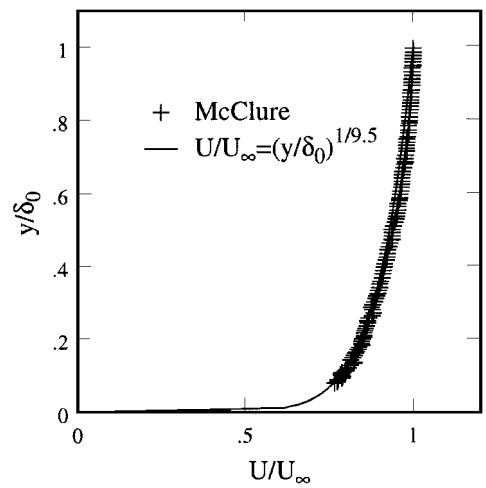

Fig. 2 Boundary-layer velocity profile.

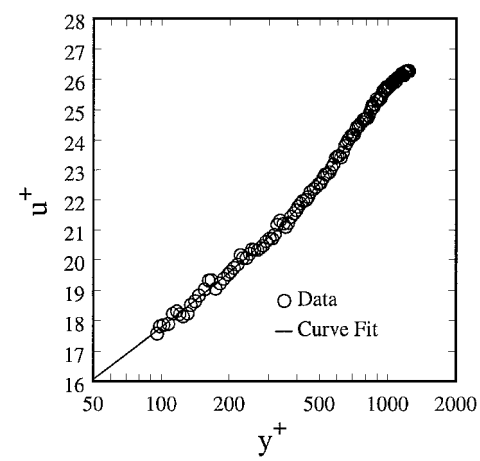

Fig. 3 Mean velocity profile in terms of u^+ vs y^+ (from Ref. 9).

Table 1 Incoming boundary-layer parameters

Parameter	Value
$(\delta_0)_{0.99U_\infty}$	0.59 in. (1.50 cm)
$(\delta_0)_{0.99(\rho U)_\infty}$	0.70 in. (1.78 cm)
δ^*	0.26 in. (0.66 cm)
H	10.2 (10.2)
Π	0.78 (0.78)
Re_θ	2.97×10^4 (2.97×10^4)
$C_f(\times 10^4)$	7.74 (7.74)

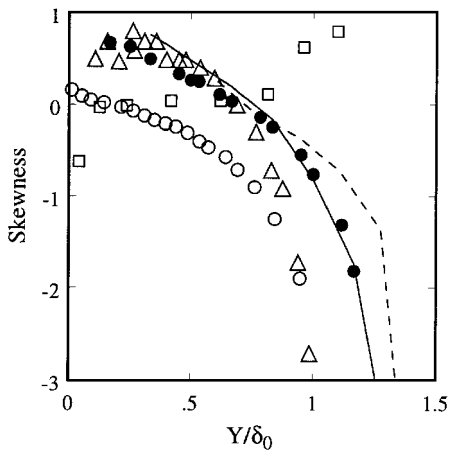

Fig. 4 Skewness coefficient across boundary layer: o, Alving, incompressible; △, Spina, $M = 2.9$ (hotwire); ●, present, $M = 5$ (hotwire); —, present, $M = 5$ (lower pitot); - - -, present, $M = 5$ (upper pitot); and □, Owen et al., $M = 7.2$ (hotwire).

several undisturbed turbulent boundary-layer parameters on the tunnel centerline at approximately the center of the instrumented plug are given in Table 1.

The skewness coefficient of the pitot-pressure fluctuations through the boundary layer is shown in Fig. 4. The results were calculated using signals from the double-tipped probe, thus the solid and hatched curves provide a measure of the repeatability of the measurements. Hot-wire data obtained in the same boundary layer were also analyzed and are also shown in Fig. 4. They agree well with the fluctuating pitot-pressure data. Also shown in Fig. 4 are the results of Alving[10] (incompressible), Spina[11] ($M = 3$), and Owen et al.[3] ($M = 7.2$) obtained from hot wires. The skewness coefficient is negative across most of the boundary layer in the incompressible case. At Mach 3 and 5 the skewness is slightly positive for $0 < Y/\delta_0 < 0.7$. Although the profiles for the incompressible, Mach 3, and Mach 5 cases show similar trends in general, the Mach 7 data of Owen et al.[3] have a different character: the skewness has negative values up to $Y/\delta_0 \approx 0.2$, approximately zero value for $0.2 < Y/\delta_0 < 0.7$ and is then positive above $Y/\delta_0 \approx 0.7$ (also note that for this data set the boundary-layer thickness δ_0 is defined as the height in the boundary layer where the pitot pressure reaches 99% of the local freestream value[2]). One observation is that the skewness profile of the Mach 7 data takes on positive values at approximately the same station at which the Mach 3 and Mach 5 data take on negative values. The reason for this discrepancy is unknown.

The flatness coefficient profiles across the boundary layer for the same data sets are given in Fig. 5. Up to $Y/\delta_0 \approx 0.6$ the subsonic data exhibit a flatness value of about 3 (Gaussian). Beyond $Y/\delta_0 \approx 0.6$ the flatness coefficient increases. In contrast, the supersonic and hypersonic data do not increase above approximately 3 until Y/δ_0 is about 0.9 or larger. Thus, the onset of intermittency in supersonic/hypersonic boundary layers occurs farther from the wall than in incompressible boundary layers. This result, which is also reported in other studies,[5,11,12] is one of the differences between incompressible/subsonic and supersonic/hypersonic boundary-layer flows. Another form of presentation, shown in Fig. 6, is one in which intermittency is defined as *3/flatness coefficient*. Note that the supersonic and hypersonic data, irrespective of the measuring techniques and Mach numbers, seem to collapse quite well for the region $0.5 < Y/\delta_0 < 0.9$.

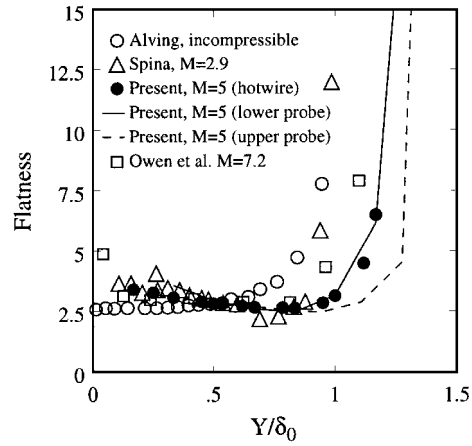

Fig. 5 Flatness coefficient across boundary layer.

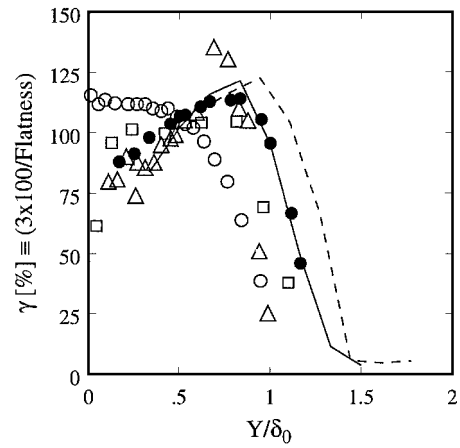

Fig. 6 Boundary-layer edge intermittency defined as 3/(flatness coefficient) (legend as in Fig. 5).

Wall-Pressure Field

Streamwise and Spanwise Length Scales

Cross correlations of the wall-pressure signals for six streamwise separation distances ranging from 0.2 to $20.9\delta_0$ are shown in Fig. 7a. The inclined dashed line in the figure shows the location of $\tau = 0$ for each streamwise separation. For clarity, each curve is shifted up by 0.1 units in $R[\Delta X, 0, 0 \mid \tau]$ relative to the one below it. With increasing separation distance the maximum correlation coefficient decreases in magnitude, and the time delay at maximum cross-correlation coefficient increases. This behavior is as expected and is a result of the pressure field gradually losing its coherence as it convects downstream. In addition to the peak correlation coefficient becoming smaller, the curves lose their sharp peaks and become broader. The corresponding coherence function curves are given in Fig. 7b. (Note that for clarity the curve for $\Delta X/\delta_0 = 16.2$ is not shown.) Although coherence, which is a measure of the degree of linear correlation between two signals, does not give any information on nonlinear relationships, it provides a qualitative interpretation of the correlation in the frequency domain. As the separation distance increases, the maximum coherence decreases, and at large separation distances only the very lowest frequencies remain coherent.

Figure 8 shows the normalized broadband convection velocity, obtained by dividing the separation distance ΔX by the time $\tau_{\max}$, at which the maximum correlation occurs. Data from other supersonic studies[1,11,13] are also shown, as are the subsonic results of Bull.[14] Note that although U_c/U_∞ asymptotes to the same value ($\approx 0.9U_\infty$) for the Mach 2.9 and Mach 5 data sets the streamwise separation in terms of δ^* at which this occurs differs by a factor of about 3, suggesting that δ^* is not the appropriate length scale. Assuming that large-scale, pressure-producing structures will retain their identity over a longer streamwise distance than small-scale structures and

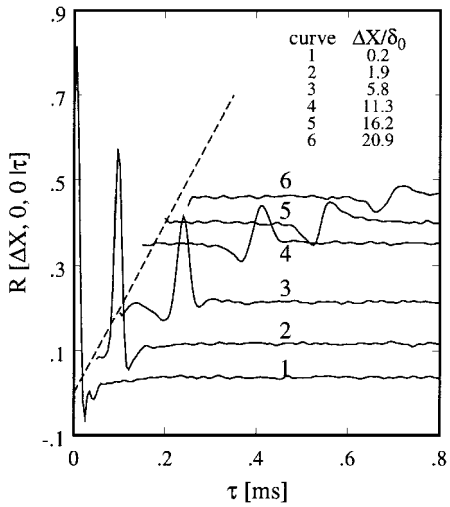

a) Wall–wall cross correlations

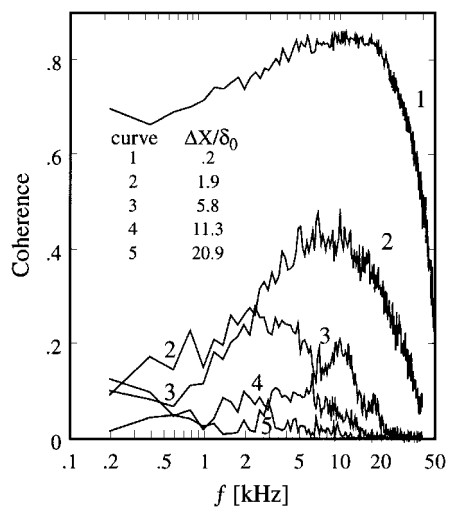

b) Corresponding coherence function plots

Fig. 7 Sample streamwise correlations.

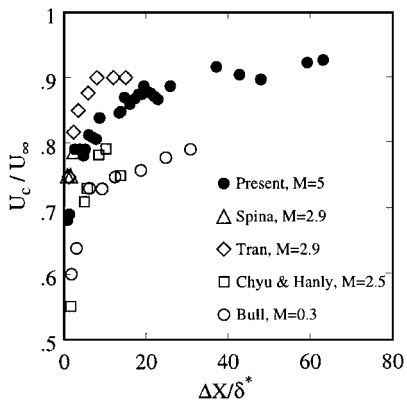

Fig. 8 Normalized convection velocity as a function of normalized streamwise spacing.

that large-scale structures are centered farther from the wall and have higher convection velocities, larger separations should correspond to higher convection velocities. An asymptotic value of $0.9U_\infty$ is physically reasonable.

The decay of the maximum cross-correlation coefficient in terms of δ_0 in the streamwise and spanwise directions is given in Figs. 9 and 10, respectively. From Fig. 9 two observations can be made immediately. First, a correlation exists for large streamwise separations (up to $15–20\delta_0$), and second, there is good agreement with other supersonic data at small separations. As far as the authors are aware, no other supersonic data are available at separations

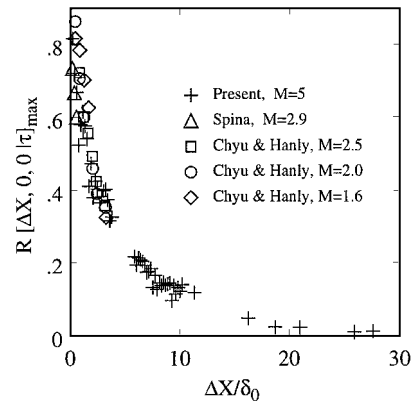

Fig. 9 Decay of maximum cross-correlation coefficient streamwise as a function of $\Delta X/\delta_0$.

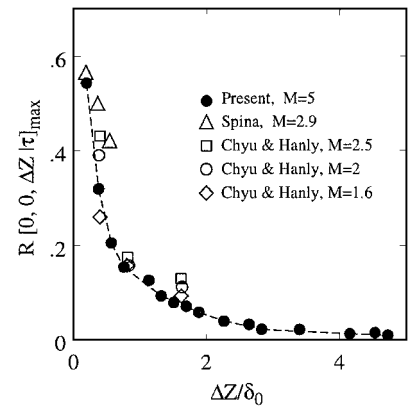

Fig. 10 Decay of maximum cross-correlation coefficient spanwise as a function of $\Delta Z/\delta_0$.

greater than about $5\delta_0$, thus the validity of δ_0 as the proper length scale is in question. In a broad sense the first observation is consistent with Owen and Horstmann's observation[2] using hot wires at Mach 7.2 that "the larger eddies persist for downstream distances of the order of $50\delta_0$." For the spanwise case (Fig. 10) the results of the present study show that a correlation exists up to a separation of $2–3\delta_0$. The agreement with other supersonic data from the literature is good, although no other results appear to be available beyond $\Delta Z/\delta_0 \approx 1.5$. Because fluctuating pitot-pressure measurements by the current authors[15–17] (and hot-wire data of Spina's[11] at Mach 2.9) show that the turbulent structure has a spanwise scale of order $0.5\delta_0$, this result is somewhat confusing. It raises the question of whether the wall-pressure correlation at larger separations is generated by turbulent structures or some other mechanism(s). This same question is also raised by Fig. 11, which shows cross-correlation results for four different situations. Two of the curves (1 and 3) are from transducers separated streamwise only whereas the other two (2 and 4) are from transducers separated streamwise and spanwise. The normalized spanwise separation $\Delta Z/\delta_0$ for curves 2 and 4 is 1.6. Comparison of curve 1 with curve 3 shows no unusual features; as was just described, there is a rapid decrease in cross-correlation magnitude with increasing streamwise separation, which is the characteristic behavior of turbulent structures. However, the small, but nonzero value of the maximum cross-correlation coefficient for curves 2 and 4, and the fact that the decrease in cross-correlation magnitude is small as $\Delta X/\delta_0$ increases from 2.5 to 8.9 suggests that the cause is probably not turbulent structures. This issue was addressed by the authors in a separate experimental study, the results of which are reported in Refs. 6 and 15–17. In brief, an experiment was conducted in which the spanwise separation between two transducers was held fixed while the pair was systematically shifted across the tunnel floor. A very small, but systematic variation in the cross-correlation maximum, with a period of about $2\delta_0$, was observed. Based on the fact that a deliberately created vortex pattern (obtained using vortex generators of different types placed upstream of the transducer array) caused a similar variation in

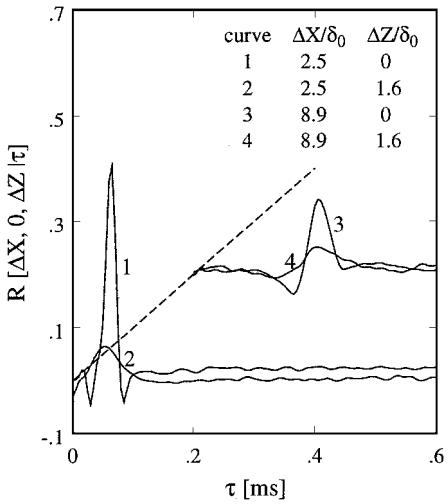

Fig. 11 Cross correlations for transducers separated spanwise and streamwise.

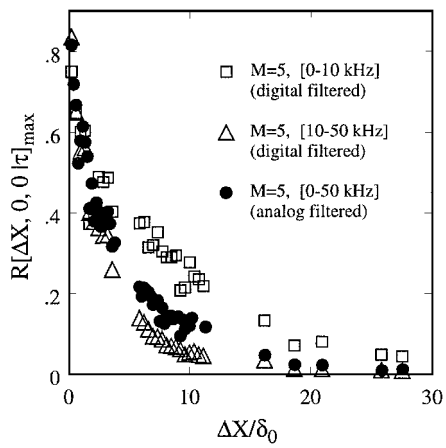

Fig. 12 Decay of maximum cross-correlation coefficient streamwise as a function of $\Delta X/\delta_0$ for different bandwidths.

cross-correlation maximum, it was inferred that there exists a weak, naturally occurring vortex structure in the undisturbed tunnel floor boundary layer. The suggestion was made, but not proven, that these naturally occurring vortex structures might be Görtler vortices.[15,16] The long tail of the spanwise decay curve of the fluctuating wall-pressure field may be related to this phenomenon.

Low/High-Frequency Components of the Wall-Pressure Field

Examination of Figs. 9 and 10 raised the question of whether some low-frequency phenomenon in the flowfield (or in the recorded signals), which becomes relatively more significant with increasing separation distance, may contribute to the correlation at larger separations. First, to determine whether electronic noise in the data acquisition system played any role at all, data were taken without flow in the test section. There was zero correlation between any pairs of spanwise-positioned transducers. Second, to explore the relative contributions of the high- and low-frequency components, the fluctuating pressure signal was high-pass and low-pass filtered. Figure 12 shows the decay of the maximum cross-correlation coefficient of the pressure signal for two different frequency ranges: (0–10-kHz) low pass and (10–50-kHz) high pass. The physical justification for this choice, as was stated earlier, is based on the assumption that large-scale structures in the boundary layer may range from 1 to $4\delta_0$ in extent. In this sense the high-pass component reflects the pressure signals of the large-scale turbulent structures.

As can be seen in Fig. 12, the maximum correlation coefficient of the high-frequency component of the signal decays faster than the low-frequency component. The decay curve for the unfiltered data (0–50 kHz) lies between the curves of the high-frequency and low-frequency components. It appears that the earlier observation based on Fig. 9 (i.e., correlation exists up to $15–20\delta_0$) does not reflect

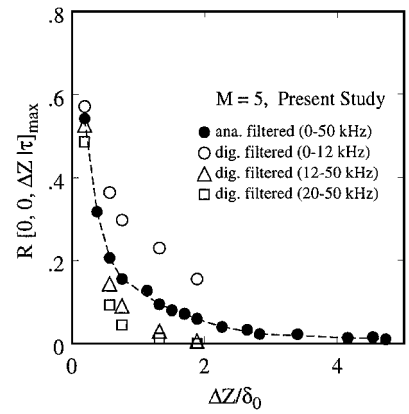

Fig. 13 Decay of maximum cross-correlation coefficient spanwise as a function of $\Delta Z/\delta_0$ for different bandwidths.

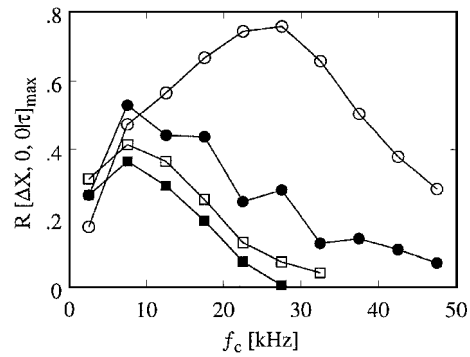

Fig. 14 Maximum cross-correlation cofficient streamwise as a function of bandwidth: o, $\Delta X/\delta^* = 1.7$; ●, $\Delta X/\delta^* = 8.2$; □, $\Delta X/\delta^* = 13.4$; and ■, $\Delta X/\delta^* = 16$.

the lifetime of the large-scale structures, unless the extent of these structures is far in excess of the $4\delta_0$ just used. The same analysis was performed for the spanwise case (Fig. 13), and the results show that low-frequency and high-frequency components of the signal also have very different decay characteristics. The digitally filtered data (20–50 kHz) indicate a decay distance of order $0.5\delta_0$ (defined roughly by $R_{\max} \approx 0.1$, as was also assumed by Spina), which is consistent with experimental flowfield measurements using hot-wire pairs (such as those of Spina[11]) as well as with the fluctuating pitot probe measurements by the current authors.[15–17]

The comments made about Fig. 12 are also supported by Fig. 14 in which the maximum cross-correlation coefficient obtained in different frequency bands is plotted vs the center of that frequency band. The fluctuating pressure signal, which has an analog frequency range of (0–50 kHz), was band-pass-filtered with a bandwidth of 5 kHz. Thus, the data were divided into 10 different frequency bands, namely, (0–5 kHz), (5–10 kHz), etc. For each band conventional time series analysis was applied, and the peak cross-correlation coefficient was determined. This procedure was repeated for several transducer separations. As the separation increases, the correlation becomes increasingly dominated by the low-frequency component of the signal.

This approach of dividing the pressure signal into 10 narrow-band frequency ranges was also employed in Fig. 15, which shows the streamwise decay of the maximum cross-correlation coefficient as a function of Strouhal number $\omega \Delta X/U_c(\omega)$. Instead of center frequency f_c the wave-number frequency $\omega\,(=2\pi f_c)$ is used. The present Mach 5 data (including some additional results on a flat plate) along with Bull's subsonic data[14] are plotted for various separations. Although the $R[\Delta X, 0, 0\,|\,\tau]_{\max}$ curves for different separations do not collapse at small Strouhal numbers, they do so at large Strouhal numbers. Thus, for higher values of $\omega \Delta X/U_c(\omega)$, two pressure-producing eddies of different sizes decay at the same rate and generate the same correlation coefficient. The physical separation distances over which the eddies lose their coherence are different but are proportional to the wavelengths of the eddies. Bull

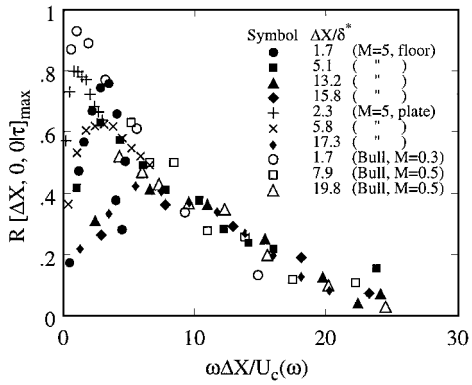

Fig. 15 Decay of maximum cross-correlation coefficient streamwise as a function of Strouhal number.

reports this proportionality factor as 4 with the assumption that a component loses its identity when the correlation value falls to 0.05. The value of 4 wavelengths is quite consistent with the results of the current work. For example, consider a component of the wall-pressure signal whose frequency is 10 kHz. This frequency is low enough for this specific structure to survive large separations. From the U_c/U_∞ vs $\Delta X/\delta^*$ plot (Fig. 8) a convection velocity of $0.9U_\infty$ seems appropriate. The corresponding wavelength of this structure is then found to be

$$\lambda = U_c(\omega)/f \approx (700\,\text{m/s})/(10{,}000\,\text{Hz}) = 0.07\,\text{m} \approx 4.7\delta_0$$

In Fig. 12 the maximum cross-correlation coefficient is given for different bandwidths. For an approximate decay length the (0–10 kHz) bandwidth can be used. The value of $R[\Delta X, 0, 0\,|\,\tau]_{\max}$ falls to 0.05 at about $25\delta_0$. Keeping in mind that only the 10 kHz structure is of interest, the decay length could be approximated with a reasonable $20\delta_0$. Thus, the corresponding decay length in terms of wavelength of the structure of interest can be determined as

$$\text{decay length} \approx 20\delta_0 \approx 4.3\lambda$$

Although the proportionality factor 4.3 is approximate, it is sufficient to suggest that the decay rules of the incompressible wall-pressure field also apply to the Mach 5 wall-pressure field. Figure 15 shows that a common curve is valid for incompressible, subsonic, and supersonic data for Strouhal numbers above about 5.

Length-Scale Issues

One of the questions raised earlier was whether or not the boundary-layer velocity thickness is an appropriate length scale for correlating the streamwise decay of the wall-pressure fluctuations. In earlier work Dolling and Dussauge[18] argued that the eddy life-time or "turnover time" should be proportional to the timescale of the turbulence given by $\Lambda/\sqrt{u'^2}$, where Λ is some length scale, an integral scale perhaps, and $\sqrt{u'^2}$ a typical value of the velocity fluctuations. For the majority of the flows for which wall-pressure fluctuation data exist, such parameters are not documented, and thus Dolling and Dussauge actually picked U_τ as the velocity scale and δ_0 as the length scale of the energetic eddies. Results from a number of studies[1,19–27] plotted as a function of $(X/\delta_0)(U_\tau/U_c)$ are shown in Fig. 16. The data show considerable scatter. According to Dolling and Dussauge, the curves with relatively large values correspond to cases that have limited bandwidth. Dolling and Dussauge suggested that the discrepancy between the data of Kistler and Chen[20] and the data of other studies might be due to a low signal-to-noise ratio of these measurements for which the reported rms values are the largest. The present data, also given in the figure, are quite consistent with the other supersonic data. However, from an overall perspective the parameter $(X/\delta_0)(U_\tau/U_c)$ does not seem to be the appropriate scale because of the large scatter between the curves.

The only way to reach a definitive answer regarding the validity of δ_0 alone as a length scale is through examination of detailed data from different boundary layers. Unfortunately, as far as the authors are aware, no single investigation using common instrumentation with an adequate bandwidth has been made.

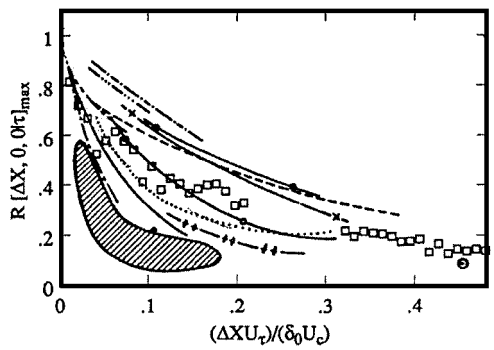

Present study	M = 4.95	□
Chyu & Hanly (Ref. 1)	M = 1.6 M = 2.0 M = 2.5	— — — —×— —●—
Muck *et al.* (Ref. 25)	M = 2.84	— - —
Speaker & Ailman (Ref. 22)	M = 3.45	- - - - - - -
Maestrello (Ref. 21)	M = 1.98 M = 3.03	—○— •••••••••••
Schewe (Ref. 19)	M = 0.02	— - —
Debieve (Ref. 23)	M = 2.3	—+ + —
Tan *et al.* (Ref. 24)	M = 2.99	— ••• —
Dussauge (Ref. 26)	M = 1.76	⊙
Bonnet (Ref. 27)	M = 2.27	———
Kistler & Chen (Ref. 20)	1.3 <M< 5	shaded zone

Fig. 16 Decay of maximum cross-correlation coefficient streamwise using scaling of Ref. 18.

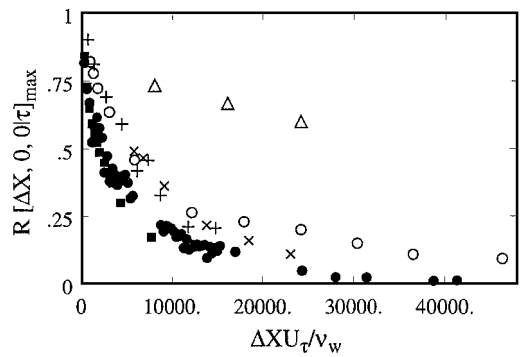

Fig. 17 Decay of maximum cross-correlation coefficient streamwise using scaling of Bull[14]: ●, $M = 5$ (present, floor); ■, $M = 5$ (present, plate); △, $M = 2.9$ (Spina[11]); ×, $M = 0.5$ (Bull); +, $M = 0.3$ (Bull); and ○, $M = 0.18$ (Willmarth and Wooldridge[28]).

An alternative scaling parameter, based on wall variables, was suggested by Bull.[14] Bull noted that when he plotted his subsonic data and the incompressible data of Willmarth and Wooldridge[28] in this form there was a fairly good collapse (Fig. 17). The data of the present study along with Spina's Mach 2.9 data[11] are also plotted. In both cases, ν is evaluated at the wall. Although for incompressible and subsonic data $\Delta X U_\tau/\nu_w$ seems to be an appropriate parameter, it does not appear so for supersonic flows. Although the friction velocity U_τ and separation distance ΔX are usually of the same order of magnitude in different supersonic flows, ν_w, which is a function of Mach number M and stagnation pressure P_0, may differ by an order of magnitude. For instance, although the wall temperature T_w and μ_w are essentially the same in the current study and that of Spina,[11] the stagnation pressure differs by a factor of 5.

Flowfield Measurements

Several flowfield experiments were conducted. They included fluctuating pitot-pressure measurements using single- and double-tipped pitot probes, a combination of wall-pressure transducers and

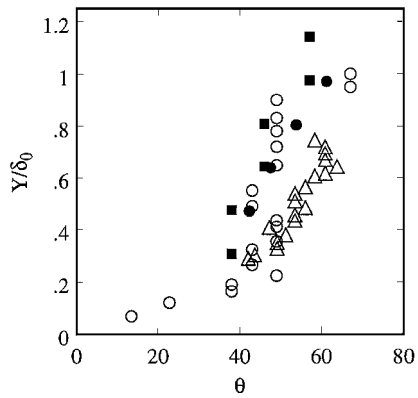

Fig. 18 Structure angle across boundary layer: ■, present, $M = 5$, $\Delta Y/\delta_0 = 0.28$, hot wire; ●, present, $M = 5$, $\Delta Y/\delta_0 = 0.28$, pitot; o, Spina,[11] $M = 2.9$, $\Delta Y/\delta_0 = 0.09$, hot wire; and △, Spina, $M = 2.9$, $\Delta Y/\delta_0 = 0.30$, hot wire.

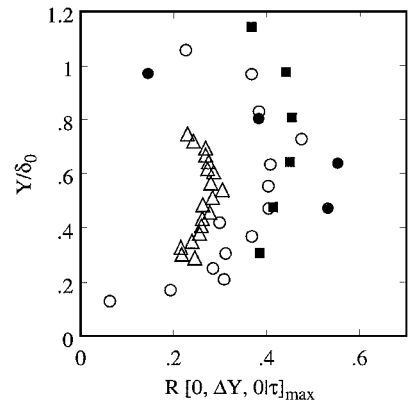

Fig. 19 Maximum cross-correlation coefficient across boundary layer: ■, present, $M = 5$, $\Delta Y/\delta_0 = 0.28$, hot wire; ●, present, $M = 5$, $\Delta Y/\delta_0 = 0.28$, pitot; o, Spina,[11] $M = 2.9$, $\Delta Y/\delta_0 = 0.20$, hot wire; and △, Spina, $M = 2.9$, $\Delta Y/\delta_0 = 0.30$, hot wire.

pitot probes, and two independent pitot probes at the same streamwise location with different spanwise and vertical separations. Hot-wire data that had been obtained in the same facility were also analyzed.

The average angles of the turbulent structures across the outer region of the boundary layer were deduced using the dual normal hot-wire and double-tipped pitot probe signals. The structure angle is given by

$$\theta = \tan^{-1}\left(\frac{\Delta Y}{U_c \tau_{\max}}\right)$$

where ΔY is the vertical distance between probe tips, U_c is the convection velocity, and $\tau_{\max}$ is the time at which the maximum correlation occurs. Figure 18 shows structure angles across the boundary layer for the Mach 3 data of Spina[11] and the present Mach 5 data. Because the structure angle is a function of the convection velocity and the accuracy of $\tau_{\max}$, which is strongly influenced by sampling frequency, there is some uncertainty in the values given. Estimates for the current fluctuating pitot-pressure data, which were acquired at 1 MHz, indicate that the uncertainty is ±3 deg in the worst case. Thus, it is fair to say that Mach 3 and Mach 5 data are in reasonably good agreement. Also the results of hot-wire measurements in the same Mach 5 boundary layer support this result (with an uncertainty of ±5 deg, the same as that of Spina's). Overall, it appears that in supersonic boundary layers the large-scale structure angles in the outer region of the boundary layer vary from about 40–60 deg, with larger values toward the edge.

Cross-correlation maxima from the current Mach 5 study and those of Spina[11] at Mach 3 are plotted in Fig. 19. For the current study the vertical separations between the tips of the probes and the wires are approximately the same ($\Delta Y/\delta_0 \approx 0.28$), whereas the vertical hot-wire separations in Spina's work are $\Delta Y/\delta_0 \approx 0.30$ and 0.20. Examination of the maximum cross-correlation coefficients at Mach 5 shows that there are some substantial differences between pitot and hot-wire cross-correlation maxima especially toward the edge of the boundary layer. A comparison of the Mach 5 and Mach 3 hot-wire data for a vertical spacing of $\Delta Y/\delta_0 \approx 0.30$ shows that the maximum cross-correlation coefficient is higher for the Mach 5 flow, suggesting that the turbulent structures in the Mach 5 boundary layer are somewhat larger than those at Mach 3.

Conclusion

Fluctuating wall-pressure measurements have been made under a Mach 5 turbulent boundary layer for streamwise transducer separations of up to $28\delta_0$ and spanwise separations up to $4.5\delta_0$. These data, in conjunction with data from other studies (all with smaller ranges of transducer separations), have been examined in an attempt to determine the parameter(s) that correlate the decay of the maximum cross-correlation coefficient of the pressure signal pairs. The sparseness of the database has made this task particularly difficult and highlight the need for additional experimental data in different boundary layers. Nevertheless some conclusions can be drawn from the available data. For streamwise separations less than about five boundary-layer thicknesses, the maximum correlation coefficient can be collapsed in terms of separation distance divided by boundary-layer thickness. The maximum cross-correlation coefficient for incompressible, subsonic, and supersonic boundary layers can also be collapsed in terms of a Strouhal number, for Strouhal numbers greater than about 5. In this case the Strouhal number is based on streamwise separation distance, narrow-band frequency, and structure convection velocity within that narrow band. For larger separations the database is too sparse to draw a definitive conclusion. The large spanwise decay distance of the maximum cross-correlation coefficient appears to be related to a weak, naturally occurring vortex pattern, possibly Görtler vortices induced in the wind-tunnel nozzle. Experimental investigation of such a phenomenon will be extremely challenging, particularly if the vortex pairs meander, as has been observed at lower speeds. Fluctuating pitot-pressure measurements were also made and analyzed in conjunction with hot-wire data obtained in the same facility and with hot-wire measurements at Mach 3. The boundary-layer large-scale structure angles, spanwise scale, and intermittency distributions agree well with results at Mach 3. Based on the higher values of the cross-correlation coefficient in the Mach 5 flow, turbulent structures appear to be somewhat larger than those at Mach 3.

Acknowledgments

Support for this research has been provided through grants from the U.S. Army Research Office (DAAL03-91-G-0023) monitored by T. Doligalski and from NASA Langley Research Center (NAG1-1471) monitored by W. E. Zorumski. These sources of support are gratefully acknowledged. The authors would also like to thank Leon Brusniak for making his hot-wire data available.

References

[1] Chyu, W. J., and Hanly, R. D., "Power and Cross-Spectra and Space-Time Correlations of Surface Fluctuating Pressures at Mach Numbers between 1.6 and 2.5," AIAA Paper 68-77, Jan. 1968.

[2] Owen, F. K., and Horstman, C. C., "On the Structure of Hypersonic Turbulent Boundary Layers," *Journal of Fluid Mechanics*, Vol. 53, Pt. 4, 1972, pp. 611–636.

[3] Owen, F. K., Horstman, C. C., and Kussoy, M. I., "Mean and Fluctuating Flow Measurements of a Fully-Developed, Non-Adiabatic, Hypersonic Boundary Layer," *Journal of Fluid Mechanics*, Vol. 70, Pt. 2, 1975, pp. 393–413.

[4] Smits, A. J., Spina, E. F., Alving, A. E., Smith, R. W., Fernando, E. M., and Donovan, J. F., "A Comparison of the Turbulence Structure of Subsonic and Supersonic Boundary Layers," *Physics of Fluids A*, Vol. 1, No. 11, 1989, pp. 1865–1875.

[5] Spina, E. F., Smits, A. J., and Robinson, S. K., "The Physics of Supersonic Turbulent Boundary Layers," *Annual Review of Fluid Mechanics*, Vol. 26, 1994, pp. 287–319.

[6] Ünalmis, Ö. H., "Structure of the Supersonic Turbulent Boundary Layer and Its Influence on Unsteady Separation," Ph.D. Dissertation, Dept. of Aerospace Engineering and Engineering Mechanics, Univ. of Texas, Austin, TX, Aug. 1995.

[7]Settles, G. S., "An Experimental Study of Compressible Turbulent Boundary Layer Separation at High Reynolds Numbers," Ph.D. Dissertation, Dept. of Mechanical and Aerospace Engineering, Princeton Univ., Princeton, NJ, Sept. 1975.

[8]Sun, C. C., and Childs, M. E., "A Modified Wall-Wake Velocity Profile for Turbulent Compressible Boundary Layers," *Journal of Aircraft*, Vol. 10, No. 6, 1973, pp. 381–383.

[9]McClure, W. B., "An Experimental Study of the Driving Mechanism and Control of the Unsteady Shock Induced Turbulent Separation in a Mach 5 Compression Corner Flow," Ph.D. Dissertation, Dept. of Aerospace Engineering and Engineering Mechanics, Univ. of Texas, Austin, TX, Aug. 1992.

[10]Alving, A. E., "Boundary Layer Relaxation from Convex Curvature," Ph.D. Dissertation, Dept. of Mechanical and Aerospace Engineering, Princeton Univ., Princeton, NJ, June 1988.

[11]Spina, E. F., "Organized Structures in a Supersonic Turbulent Boundary Layer," Ph.D. Dissertation, Dept. of Mechanical and Aerospace Engineering, Princeton Univ., Princeton, NJ, Oct. 1988.

[12]Robinson, S. K., "Space-Time Correlation Measurements in a Compressible Turbulent Boundary Layer," AIAA Paper 86-1130, May 1986.

[13]Tran, T. T., "An Experimental Investigation of Unsteadiness in Swept Shock Wave/Turbulent Boundary Layer Interactions," Ph.D. Dissertation, Mechanical and Aerospace Engineering Dept., Princeton Univ., Princeton, NJ, March 1987.

[14]Bull, M. K., "Wall-Pressure Fluctuations Associated with Subsonic Turbulent Boundary Layer Flow," *Journal of Fluid Mechanics*, Vol. 28, Pt. 4, 1967, pp. 719–754.

[15]Ünalmis, Ö. H., and Dolling, D. S., "Decay of Wall Pressure Field and Structure of a Mach 5 Adiabatic Turbulent Boundary Layer," AIAA Paper 94-2363, June 1994.

[16]Ünalmis, Ö. H., and Dolling, D. S., "On the Possible Relationship Between Low Frequency Unsteadiness of Shock-Induced Separated Flow and Görtler Vortices," AIAA Paper 96-2002, June 1996.

[17]Ünalmis, Ö. H., and Dolling, D. S., "Experimental Study of Causes of Unsteadiness of Shock-Induced Turbulent Separation," *AIAA Journal*, Vol. 36, No. 3, 1998, pp. 371–378.

[18]Dolling, D. S., and Dussauge, J. P., "Fluctuating Wall-Pressure Measurements," *A Survey of Measurements and Measuring Techniques in Rapidly Distorted Compressible Turbulent Boundary Layers*, AGARDograph 315, AGARD, Nov. 1988, Chap. 8.

[19]Schewe, G., "On the Structure and Resolution of Wall Pressure Fluctuations Associated with Turbulent Boundary Layer Flow," *Journal of Fluid Mechanics*, Vol. 134, 1983, pp. 311–328.

[20]Kistler, A. L., and Chen, W. S., "The Fluctuating Pressure Field in a Supersonic Turbulent Boundary Layer," Jet Propulsion Lab., JPL-TR-32-277, California Inst. of Technology, Pasadena, CA, Aug. 1962.

[21]Maestrello, L., "Radiation from and Panel Response to a Supersonic Turbulent Boundary Layer," Boeing Scientific Research Labs., D1-82-0719, Seattle, WA, Sept. 1968.

[22]Speaker, W. V., and Ailman, C. M., "Spectra and Space-Time Correlations of the Fluctuating Pressures at a Wall Beneath a Supersonic Turbulent Boundary Layer Perturbed by Steps and Shock Waves," NASA CR-486, May 1966.

[23]Debieve, J. F., "Etude d'une Interaction Turbulence—Onde de Choc," Ph.D. Dissertation, Institut de Mecanique Statistique de la Turbulence, Univ. Aix-Marseille II, Marseille, France, June 1983.

[24]Tan, D. K. M., Tran, T. T., and Bogdonoff, S. M., "Surface Pressure Fluctuations in a Three Dimensional Shock Wave/Turbulent Boundary Layer Interaction," AIAA Paper 85-0125, Jan. 1985.

[25]Muck, K. C., Dussauge, J. P., and Bogdonoff, S. M., "Structure of the Wall Pressure Fluctuations in a Shock-Induced Separated Flow," AIAA Paper 85-0179, Jan. 1985.

[26]Dussauge, J. P., "The Relaxation of a 'Relaminarized' Turbulent Boundary Layer in Supersonic Flow," *Proceedings of the 5th Turbulent Shear Flow Symposium*, A86-30201 13-34, Cornell Univ., Ithaca, NY, 1985.

[27]Bonnet, J. P., "Space-Time Correlations of Wall Pressure Fluctuations in Shock-Induced Separated Turbulent Flows," *Physics of Fluids*, Vol. 31, No. 10, 1988, pp. 2821–2833.

[28]Willmarth, W. W., and Wooldridge, C. E., "Measurements of the Fluctuating Pressure at the Wall Beneath a Thick Boundary Layer," *Journal of Fluid Mechanics*, Vol. 14, Pt. 2, 1962, pp. 187–210.

S. K. Aggarwal
Associate Editor